

Lensed or not lensed: Determining lensing magnifications for binary neutron star mergers from a single detection

Peter T. H. Pang,^{1,2,*} Otto A. Hannuksela,^{1,2,†} Tim Dietrich,^{3,1} Giulia Pagano,^{4,5,‡} and Ian W. Harry⁶

¹*Nikhef – National Institute for Subatomic Physics, Science Park, 1098 XG Amsterdam, The Netherlands*

²*Department of Physics, Utrecht University, Princetonplein 1, 3584 CC Utrecht, The Netherlands*

³*Institute for Physics and Astronomy, University of Potsdam,*

Karl-Liebknecht-Str. 24/25, 14476, Potsdam, Germany

⁴*Dipartimento di Fisica “Enrico Fermi”, Università di Pisa, Pisa I-56127, Italy*

⁵*INFN sezione di Pisa, Pisa I-56127, Italy*

⁶*Institute for Cosmology and Gravitation, University of Portsmouth, 1-8 Burnaby Road, Portsmouth, P01 3FZ, UK*

(Dated: February 13, 2020)

Advanced LIGO and Advanced Virgo could observe the first lensed gravitational wave sources in the coming years, while the future Einstein Telescope could observe hundreds of lensed events. It is, therefore, crucial to develop methodologies to distinguish between lensed from unlensed gravitational-wave observations. A lensed signal not identified as such will lead to biases during the interpretation of the source. In particular, sources will appear to have intrinsically higher masses. No robust method currently exists to distinguish between the magnification bias caused by lensing and intrinsically high-mass sources. In this work, we show how to recognize lensed and unlensed binary neutron star systems through the measurement of their tidal effects for highly magnified sources as a proof-of-principle. The proposed method could be used to identify lensed binary neutron stars, which are the chief candidate for lensing cosmography studies. We apply our method on GW190425, finding no clear evidence for or against lensing, mainly due to the poor measurement of the event’s tidal effects. However, we expect that future detections with better tidal measurements can yield better constraints.

I. INTRODUCTION

Between 2015 and 2017, Advanced LIGO [1] and Advanced Virgo [2] conducted their first two observation runs (O1 and O2) detecting several binary black hole (BBH) mergers and one binary neutron star (BNS) merger [3]. The third observation run (O3) is currently on-going and numerous candidate gravitational transients have been observed [4, 5]. Future observing runs will see upgrades to the Advanced LIGO detectors and the Advanced Virgo detector, and, in addition, the Japanese observatory KAGRA [6–8] is expected to join the network in 2020 [9].

When gravitational waves (GWs) travel near a galaxy or a galaxy cluster, their trajectories are curved, resulting in strong gravitational lensing [10–17]. The lensing magnifies the amplitude of the waves without changing their frequency evolution [18, 19]. In the case of strong lensing by galaxies, it is possible to produce multiple “images”, which would arrive to us with relative time-delays between minutes and weeks¹ [22, 23]. Based on predictions on the number of expected GW sources, and the distribution of lenses in the Universe, Refs. [24–26] suggest that lensed gravitational-waves may be detected in the coming years, as the LIGO/Virgo detectors reach their design sensitivities.² The number of de-

tectable events could reach hundreds in the Einstein Telescope [27, 28]. Lensed GWs present several potential applications in fundamental physics, astrophysics, and cosmology [22, 29–35].

A number of possibilities to identify a lensed GW signal have been proposed. One can look for signatures of multiple images or microlensing within GW data [23, 29, 36–40]. Alternatively, one could search for a population of apparently high-mass binary events produced by lensing magnification [19, 26, 41]. The first combined search for all these signatures was performed recently on the O1/O2 data [42].

Here we focus on the problem of reliably identifying lensed binary neutron star signals. The overall magnification caused by lensing is degenerate with the luminosity distance measured from the GW signal and so a lensed system will appear to be closer than it truly is [19, 24, 26, 41]. As the distance to the binary is biased, the estimation of the redshift to the binary will be as well. A redshifted gravitational-wave signal will appear to an observer to have higher masses than in reality.

The recent high-mass BNS detection, GW190425 [43], is therefore of particular interest. The mass of the system is higher than expected from the known galactic double neutron star population [44, 45]. Could this signal be a lensed system consistent with the known population? Unfortunately, to answer this question definitively, we would need a unique signature to discern an intrinsically high-mass binary event from a lensed event.

We note that the problem could, in principle, be resolved by lens statistics: the lensed hypothesis is disfavored *a priori*,

* thopang@nikhef.nl

† o.hannuksela@nikhef.nl

‡ giulia.pagano@pi.infn.it

¹ Let us note gravitational lensing by galaxy clusters could produce time-delays as large as months to years [20, 21]. However, we do not consider this scenario here, as lensing by galaxy cluster is considered to be less likely (see, e.g., [17, 21]).

² Specifically, Refs. [24–26] arrive at $\sim 0.1 - 10 \text{ yr}^{-1}$ observable lensed

events per year.

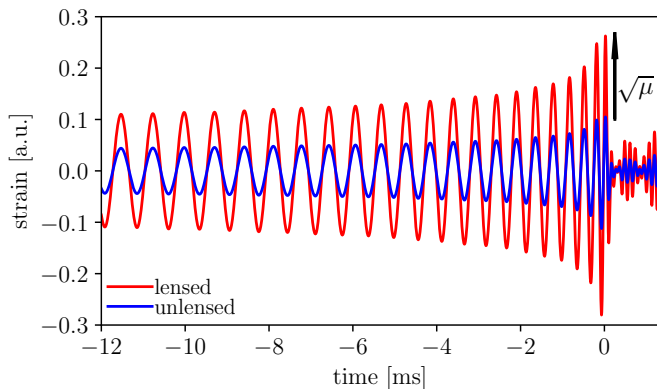


FIG. 1. *Illustration of amplitude magnification*: GW strain of a lensed (red) and unlensed (blue) signal from an example binary neutron star system. The waveform is adjusted from a numerical relativity simulation performed by the CoRe collaboration with the BAM code [47].

as the rate of lensed BNSs is low within LIGO/Virgo [46]. However, the prior probability of the other hypothesis (a new population of BNSs) is largely unknown, as the masses are inconsistent with the observed double neutron star population within the galaxy [44, 45]. Without a good grasp of the relative prior probabilities of the two hypotheses, a quantitative comparison is challenging.

In this work, we propose a robust method to rule out or confirm the lensing hypothesis for BNSs. While GW lensing biases the intrinsic mass measurement, it does not bias the tidal deformabilities as measured from the GW phasing. Therefore, a lensed binary would appear as a high-mass source with the tidal deformability of a lower-mass binary. We demonstrate, for the first time, that this can be used as a smoking-gun evidence of lensing, or as a way to rule out the hypothesis.

Besides eliminating magnification bias, detecting lensing will be important especially for BNS systems, considering that most strong lensing cosmography studies (such as measurements of the Hubble constant, accurate tests of the speed of gravity and polarization tests) require an electromagnetic counterpart [30–34].

The article is structured as follows. In Sec. II, we describe how lensing will effect the gravitational wave signal observed from a BNS merger. Sec III introduces the methodology to break the degeneracy between magnification and distance measurement via the tidal deformation of a BNS. Sec IV compares the recovery of magnification between the tidal measurement and assumed binary mass population from simulated signals. We then apply our methods to GW190425, finding no significant evidence favoring the lensed or unlensed scenario (with a log Bayes factor $\log \mathcal{B}_{\mathcal{U}}^{\mathcal{L}} = -0.608_{-0.021}^{+0.046}$), and constraining the lensing magnification $\mu \leq 86.5_{-11.2}^{+0.5}$. Finally, we provide an outlook for future lensed gravitational-wave detections in Sec. VI.

II. BINARY NEUTRON STAR LENSING

The GW signal of a non-eccentric BNS coalescence is completely described by its components’ masses $m_{1,2}$, spins $\vec{s}_{1,2}$ and the supranuclear equation of state(s) governing the internal physics of both neutron stars. There are a number of ways in which a signal emitted by a BNS system will differ from a BBH system with the same masses and spins, due to the presence of matter. These include the complex post-merger signal [48–53], the deformation of the neutron stars due to tidal forces [54, 55], and the deformation of the neutron stars due to their own rotation [56–58]. Of these effects, the deformation of the neutron star due to tidal forces provides the best measurable constraint on the internal structure and equation of state [59, 60]. The tidal deformability determines the deformation of each neutron star in the gravitational field of the companion and is quantified by the parameter [54, 61]

$$\Lambda = \frac{2}{3} k_2 \left(\frac{R}{m} \right)^5, \quad (1)$$

where k_2 , m , R are the 2nd Love number, the mass, and the radius of the individual neutron stars, respectively. The tidal deformability as a function of mass can be obtained by solving the TOV equation [62] with a given EOS. These parameters depend strongly on the equation of state.

When a gravitational wave signal is lensed by intervening galaxies or galaxy clusters, the lensing magnifies the signal, increasing its amplitude without changing the signal morphology; cf. Fig. 1. The effect is degenerate with the luminosity distance as measured from the gravitational-waves [24]

$$D^{\text{est}} = \frac{D}{\mu}, \quad (2)$$

where D^{est} and D are the observed and true luminosity distances, respectively, and μ is the magnification induced by gravitational lensing. The measured redshift $z^{\text{est}} \equiv z(D^{\text{est}})$ is therefore also biased³. Redshift will cause a shift in the observed masses of the signal according to

$$m_i = \frac{m_i^{\text{est}}}{1+z}, \quad (3)$$

where m_i^{est} is the observed mass of each component. Therefore in the case of a lensed source not including the lensing magnification when characterizing the source will bias the inferred distance, redshift and mass of the system.

Since the gravitational-wave morphology is unchanged by lensing (Fig. 1), the parameters which we directly infer from the gravitational-wave phasing are unchanged [16].⁴ That is,

³ The luminosity distance (either observed or intrinsic) is related to redshift under the assumption of standard Λ CDM cosmology [63].

⁴ Let us note that Ref. [64] suggested that when the GW passes through a lensing saddle point, the signal morphology could exhibit a minor change. It was suggested that this could lead to a bias of 45 deg in the orbital line-

among others, the detector-frame masses $m_{1,2}^{\text{det}}$ and the observed tidal deformabilities $\Lambda_{1,2}$, which are redshift independent [65], both remain unbiased. At leading order, the individual tidal deformabilities enter the GW phasing in a mass-weighted average $\tilde{\Lambda}$, which is given by

$$\tilde{\Lambda} = \frac{8}{13} \left((1 + 7\eta - 31\eta^2)(\Lambda_1 + \Lambda_2) + \sqrt{1 - 4\eta}(1 + 9\eta - 11\eta^2)(\Lambda_1 - \Lambda_2) \right), \quad (4)$$

where $\eta \equiv m_1 m_2 / (m_1 + m_2)^2$ is the symmetric mass ratio. Because the tidal effects can be *estimated* from the masses, we will obtain two independent measurements of the tidal effects: First, the unbiased measurement of Λ_i directly from the waveform phasing. Secondly, the *estimated* $\Lambda_i^{\text{est}} = \Lambda(m_i)$, from the estimate of the masses, combined with Eq. 1.

By making use of the above definitions, the hypothesis that the source is lensed

$$\begin{aligned} \mathcal{H}_L : p(\mu) &\propto \mu^{-3}, \\ D &= \sqrt{\mu} D^{\text{est}}, \\ z &= z(\sqrt{\mu} D^{\text{est}}), \\ m_i &= \frac{m_i^{\text{det}}}{1+z} = m_i^{\text{est}} \frac{1+z^{\text{est}}}{1+z}, \\ \Lambda_i^{\text{est}} &= \Lambda(m_i) = \Lambda \left(m_i^{\text{est}} \frac{1+z^{\text{est}}}{1+z} \right), \end{aligned} \quad (5)$$

and, similarly, the hypothesis that the source is unlensed

$$\begin{aligned} \mathcal{H}_U : m_i &= m_i^{\text{est}}, \\ D &= D^{\text{est}}, \\ \Lambda_i^{\text{est}} &= \Lambda(m_i) = \Lambda(m_i^{\text{est}}), \end{aligned} \quad (6)$$

where $z(D)$ is the redshift as a function luminosity distance D with a cosmological model given. That is, in the lensed hypothesis, the estimated masses and distances will be biased by the magnification, whereas in the unlensed one, they are their intrinsic (source-frame) quantities. We assume a high-magnification prior $p(\mu) \propto \mu^{-3}$, which is generally a power-law near caustics [66].

Consequently, the effect of the lensing magnification is to increase the observed source-frame masses, while the measured tidal deformability remains unchanged. This is illustrated in Figure 2, where we simulate a BNS source with a luminosity distance of $D^{\text{est}} = 100\text{Mpc}$ and source-frame masses (1.35, 1.35), with and without lensing magnification.

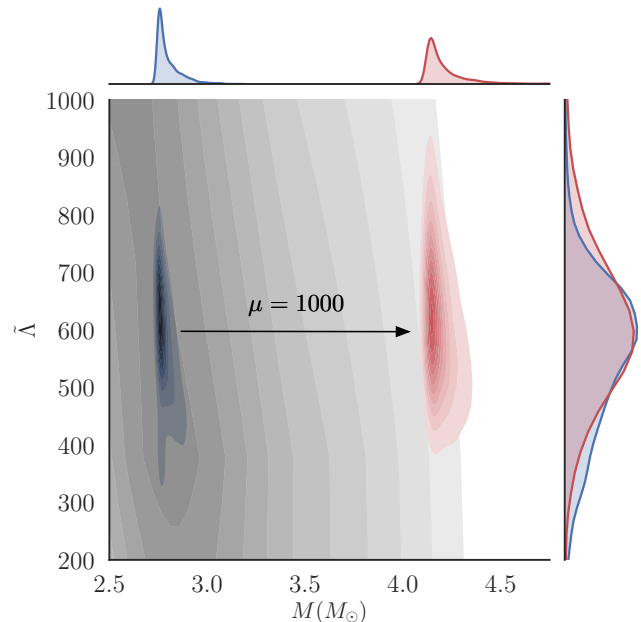


FIG. 2. *Effect of lensing on inferred parameters:* Corner plot of the posterior distribution of the estimated source total mass M and the tidal deformability $\tilde{\Lambda}$ of the same binary neutron star merger with (red) and without (blue) magnification. The plot demonstrates the effect of lensing on a binary neutron star merger signal. It biases the estimated source mass to larger values without affecting the observed tidal deformability. The expected distribution of $\tilde{\Lambda}$ - M with the ENG EOS [67] is also shown (grey), the increase of the estimated source mass due to lensing creates tension between the expected and measured values of $\tilde{\Lambda}$ - M .

III. BREAKING THE LENSING DEGENERACY

The tidal deformability of a BNS can be obtained in three ways: directly from the gravitational-wave phasing measurement, e.g. [3, 61, 68], from the observation of electromagnetic counterparts [69–74], or from the measured masses $m_{1,2}$ under the assumption of a given (known) EOS.

Unfortunately, despite recent advances, the exact equation of state (EOS) governing the interior of neutron stars, i.e., cold matter at supranuclear densities, is still unknown. Information about the neutron star EOS can be obtained from nuclear physics computation, e.g., [75, 76], from the observation of radio pulsars, e.g., [77], or from the multi-messenger observation of compact binary mergers, e.g., [78]. Considering the latter, analysis of the GW signal GW170817 [79] disfavored a number of theoretically allowed EOSs, which predict large tidal deformabilities and consequently large neutron star radii. Meanwhile, the electromagnetic observation of AT2017gfo and sGRB170817 [80–94] disfavored EOSs with too small tidal deformabilities, i.e., too soft EOSs [78]. In the future, with a growing number of multi-messenger detections of BNS mergers, and additional experiments, e.g. NICER [95], constraints on the allowed range of EOSs will greatly improve.

Given an EOS, the posterior distribution of tidal deforma-

of-sight, and possibly minor changes in the phasing for eccentric binaries and in the higher modes of merger/ringdown. We have neglected such potential effects as we consider only the inspiral part where the morphology is likely to be unchanged. However, they could be included by convolving the waveform with the complex magnification in a future study.

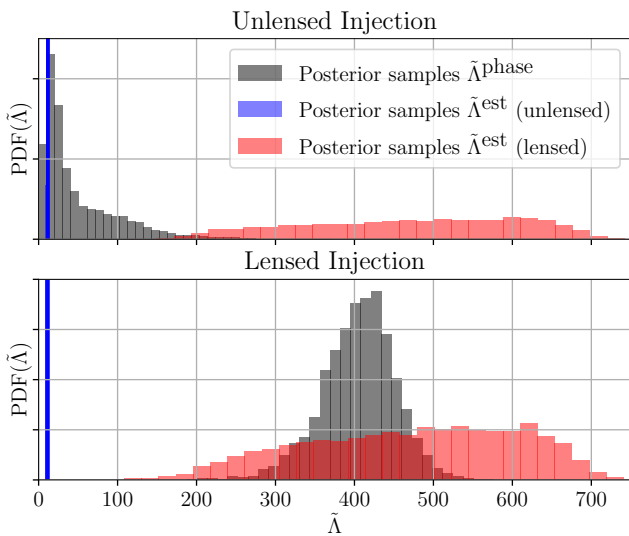


FIG. 3. *Effect of lensing on the estimated tidal deformability*: The posterior distribution of the tidal deformability as estimated from the gravitational-wave phasing (gray), and the binary masses under the unlensed and lensed hypothesis (blue and red, respectively). In the unlensed case (top panel), the posterior measurement, as estimated from the gravitational-wave phasing, overlaps with the unlensed prediction (blue), favoring the unlensed hypothesis. Vice versa, in the lensed case (bottom panel), the posterior measurement (gray) overlaps with the lensed prediction (red), supporting the lensed hypothesis. The intrinsic binary masses $m_1 = m_2 = 2.02 M_\odot$ ($m_1 = m_2 = 1.35 M_\odot$) for the unlensed (lensed) case, while the estimated masses $m_1^{\text{est}} = m_2^{\text{est}} = 2.02 M_\odot$ in both cases. In this illustration, we assume SFHo equation of state [96] and assume fixed magnification $\mu = 1000$ to allow for a clear visual illustration. We show the case with variable magnification in Fig. 5.

bilities as estimated from the (observed) binary component masses under the *unlensed* hypothesis is

$$p(\Lambda_i^{\text{est}}|d, \text{EOS}, \mathcal{H}_U) = \int dm_i^{\text{det}} dz^{\text{est}} \delta(\Lambda_i^{\text{est}} - \Lambda(m_i^{\text{est}})) \times p(m_i^{\text{det}}, z^{\text{est}}|d, \mathcal{H}_U), \quad (7)$$

The joint posterior $p(m_i^{\text{est}}, z^{\text{est}}|d)$ is the posterior inferred by LALInference. If the event is lensed, the lensing biases the tidal deformability under the unlensed hypothesis $p(\Lambda_i^{\text{est}}|d, \text{EOS}, \mathcal{H}_U)$, as predicted from the EOS, towards smaller values (as described in Sec. II).

When lensing at a given magnification is taken into account, the tidal deformability estimate becomes

$$p(\Lambda_i^{\text{est}}|d, \mu, \text{EOS}, \mathcal{H}_L) = \int dm_i^{\text{det}} dz \delta\left(\Lambda_i^{\text{est}} - \Lambda\left(\frac{m_i^{\text{det}}}{1+z}\right)\right) \times p(m_i^{\text{det}}, z|d, \mathcal{H}_L), \quad (8)$$

where

$$p(m_i^{\text{det}}, z|d, \mu, \mathcal{H}_L) = \int dD^{\text{est}} \delta(z - z(\sqrt{\mu}D^{\text{est}})) \times p(m_i^{\text{det}}, D^{\text{est}}|d, \mathcal{H}_L). \quad (9)$$

EOS	Lensed ($\mu = 1000$)	Unlensed ($\mu = 1$)
SFHo	(1.35, 432.94)	(2.02, 11.84)
ENG	(1.35, 644.66)	(2.02, 24.25)

TABLE I. Summary of the source-frame mass and the tidal deformability of the simulated binary neutron star mergers. Each cell shows the source-frame mass, tidal deformability pair (m, Λ) of the injection under different EOS and lensing scenario.

However, we also obtain an *independent* posterior measurement of the tidal deformability $p(\Lambda^{\text{phase}}|d)$ directly from the gravitational-wave phasing, which is unbiased by lensing. By doing so, we can break the magnification-induced degeneracy by matching the two independent posterior measurements ($p(\Lambda^{\text{phase}}|d)$ and $p(\Lambda_i^{\text{est}}|d, \mu)$) together, and rule out or confirm lensing.

IV. DISCRIMINATING BETWEEN HIGH-MASS BINARIES AND LENSED BINARIES

Currently known binary neutron star systems, excluding GW observations, come from Galactic observations, which consists of relatively low-mass binaries where the total mass follows roughly a normal distribution with a $2.69 M_\odot$ mean and $0.12 M_\odot$ standard deviation [44]. If a high-mass BNS system was observed with GWs it could be considered that it is a lensed system consistent with the Galactic population. It would then appear as an intrinsically high-mass BNS with an apparently high tidal deformability. On the other hand, the system could belong to a new population of high-mass BNSs. If such a binary was observed, it would also appear as a high-mass BNS, but with an apparently low tidal deformability.

Let us therefore show a simple illustrative example how to distinguish between these two scenarios by use of tidal measurements. For this purpose, we simulate a gravitational-wave signal from a ($m_1 = m_2 = 1.35 M_\odot$) *lensed BNS* at $\mu = 1000$, consistent with the Galactic double neutron star population, at an observed distance of 100 Mpc, assuming LIGO/Virgo detector network at design sensitivity, and described by the SFHo[96] and ENG[67] EOSs⁵.

For our analysis, we employ the standard LVC-developed nested sampling framework, LALInference (see Appendix A and Ref. [97, 98] for details). We recover the tidal deformability from the gravitational-wave phasing (Method-I) and from the EOS and masses (Method-II) (see Fig. 3, bottom panel, gray and blue bins, respectively)⁶. The results disagree with each other, ruling out the unlensed hypothesis. Then, we assume that the event is lensed at a magnification of $\mu = 1000$, and repeat the measurement (Fig. 3, bottom panel, gray and red bins, respectively). The posteriors overlap, supporting the lensing hypothesis.

⁵ These particular EOSs are chosen since they are broadly in agreement with joint-constraint derived from GW170817 and AT2017gfo, e.g., [73, 74, 78]

⁶ We assume the SFHo EOS [96], for simplicity.

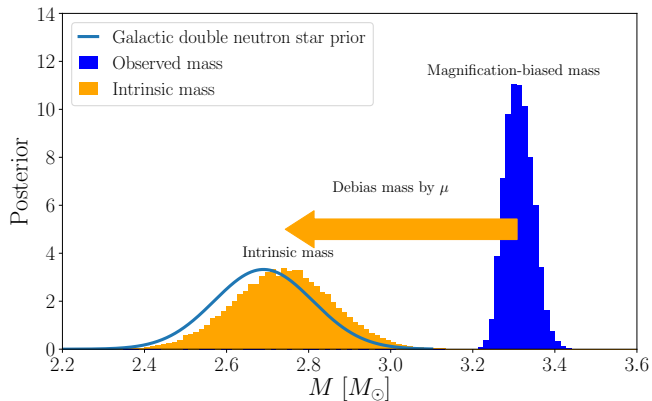


FIG. 4. Illustration of the magnification posterior computation for GW190425 from the binary masses, assuming the galactic double neutron star population as the mass prior. The figure shows the observed total binary mass for GW190425 (orange), the galactic double neutron star population prior (green), and the mass distribution if the event was lensed (blue). By re-weighting the un lensed posterior, we can estimate the lensing magnification μ under the lensing hypothesis. Note that we can also estimate the lensing magnification independently of the galactic double neutron star prior using tidal effects, as illustrated in Fig. 3.

We then demonstrate the same test for a ($m_1 = m_2 = 2 M_\odot$) *unlensed but high-mass BNS* at an observed distance D^{est} of 100 Mpc. In this case, the tidal deformability from the gravitational-wave phasing and from the EOS/masses overlap (see Fig. 3, top panel), favoring the unlensed hypothesis. Thus, the test can be used to discriminate between intrinsically high-mass BNSs and lensed BNSs. Note that here, for the sake of illustrating the method, we have fixed the magnification; we show the more general case with variable magnification below.

Let us now consider the more general case with arbitrary magnification, instead of fixed magnification. Given a source population (which we assume to be the galactic double neutron star population), we can estimate the lensing magnification $p(\mu|d, \mathcal{H}_L^{\text{DNS}})$

where we have explicitly defined the hypothesis $\mathcal{H}_L^{\text{DNS}}$ to refer to the magnification estimate from the binary *masses* (see Appendix B for the detailed derivation).⁷ This is done by *unbiasing* the GW measurement such that it is consistent with the expected source population (see Fig. 4, for an illustration of the process for GW190425).

Alternatively, we can estimate the magnification μ by combining the estimated tidal deformability with the directly mea-

sured one (see Appendix B)

$$p(\mu|d, \text{EOS}, \mathcal{H}_L^{\text{Tidal}}) \propto \left\langle \frac{p(\tilde{\Lambda}^{\text{phase}}|d, \mathcal{H}_U)}{p(\tilde{\Lambda}^{\text{phase}}|q, \mathcal{H}_U)} \mathcal{W}_{\text{EOS}} \right\rangle_{\tilde{\Lambda}^{\text{phase}} = \tilde{\Lambda}^{\text{est}}}, \quad (10)$$

where $p(\tilde{\Lambda}^{\text{phase}}|d, \mathcal{H}_U)$ is the posterior distribution of the measured tidal deformability under the unlensed hypothesis, $\tilde{\Lambda}^{\text{est}}$ is the estimated tidal deformability with a given magnification and EOS, and $\langle \dots \rangle$ refers to an average over the mass and distance posterior samples. The weight \mathcal{W}_{EOS} is given by

$$\mathcal{W}_{\text{EOS}} = \frac{p(m_1^{\text{est}}, m_2^{\text{est}}|D^{\text{est}}, \mu, \mathcal{H}_L^{\text{Tidal}}, \text{EOS})p(D^{\text{est}}|\mu, \mathcal{H}_L)}{p(m_1^{\text{est}}, m_2^{\text{est}}|D^{\text{est}}, \mathcal{H}_U)p(D^{\text{est}}|\mathcal{H}_U)} \times p(\mu|\mathcal{H}_L). \quad (11)$$

Here $\mathcal{H}_L^{\text{Tidal}}$ refers to the lensed hypothesis that additionally enforces $p(\Lambda, \Lambda^{\text{est}}|\mathcal{H}_L^{\text{Tidal}}) = p(\Lambda|\mathcal{H}_L)p(\Lambda^{\text{est}}|\mathcal{H}_L)\delta(\Lambda^{\text{est}} - \Lambda)$ in the prior, but makes no assumption on the mass prior, except that it is in the allowed EOS range.

We can calculate the evidence for the lensed hypothesis Z_L and the unlensed hypothesis Z_U by

$$\begin{aligned} Z_L &= \int d\mu p(d|\mu, \text{EOS})p(\mu|\mathcal{H}_L) \\ Z_U &= p(d|\mu = 1, \text{EOS}). \end{aligned} \quad (12)$$

The log Bayes factor $\log \mathcal{B}_U^L$ is defined as the log of the ratio between the two evidence, therefore $\log \mathcal{B}_U^L \equiv \log(Z_L/Z_U)$. A positive $\log \mathcal{B}_U^L$ shows that the lensed hypothesis is more plausible than the unlensed hypothesis. For the analysis, we consider a range of EOSs, which are SFHo, ENG and MPA1. These EOSs show agreement with the joint-constraint obtained with GW170817 and AT2017gfo [78].

Since the tidal deformability measurement is not biased by lensing, we expect this secondary measurement of the magnification to be independent of any assumptions on the source population (i.e., it is completely unbiased). Therefore, we expect the magnification to be low for unlensed binaries, and high for lensed binaries.

Fig. 5 shows the magnification posteriors evaluated via the two methods above, for both the lensed and unlensed injections with different EOSs (Table I). We observed that the required magnifications $p(\mu|d, \mathcal{H}_L^{\text{DNS}})$, as evaluated from the galactic double neutron star population, are in the $\mu \sim \mathcal{O}(100) - \mathcal{O}(1000)$ range for both the lensed and unlensed injections (Fig. 5, gray bins). Meanwhile, the magnifications as estimated from the unbiased tidal deformabilities are different for the two scenarios, favoring the unlensed case for the unlensed injection, and lensed case for the lensed injection (solid lines, for the SFHo, ENG and MPA1 EOSs). Most notably, we find that the two magnification estimates disagree in the unlensed case, ruling out the lensed hypothesis at a log Bayes factor $\log \mathcal{B}_U^L$ of $-2.72(-2.68)$, $-2.75(-2.71)$ and $-2.82(-2.83)$ for SFHo, ENG and MPA1, respectively, for SFHo(ENG) injection. And agree in the lensed case, confirming the hypothesis at a log Bayes factor $\log \mathcal{B}_U^L$ of $38.5(36.26)$, $31.2(32.63)$ and $20.9(26.75)$ for SFHo, ENG and MPA1, respectively, for SFHo(ENG) injection. For the unlensed case,

⁷ I.e., the mass prior $p(M|\mathcal{H}_L^{\text{DNS}})$ is the one for galactic double neutron stars, but we make no explicit constraint on the tidal measurements.

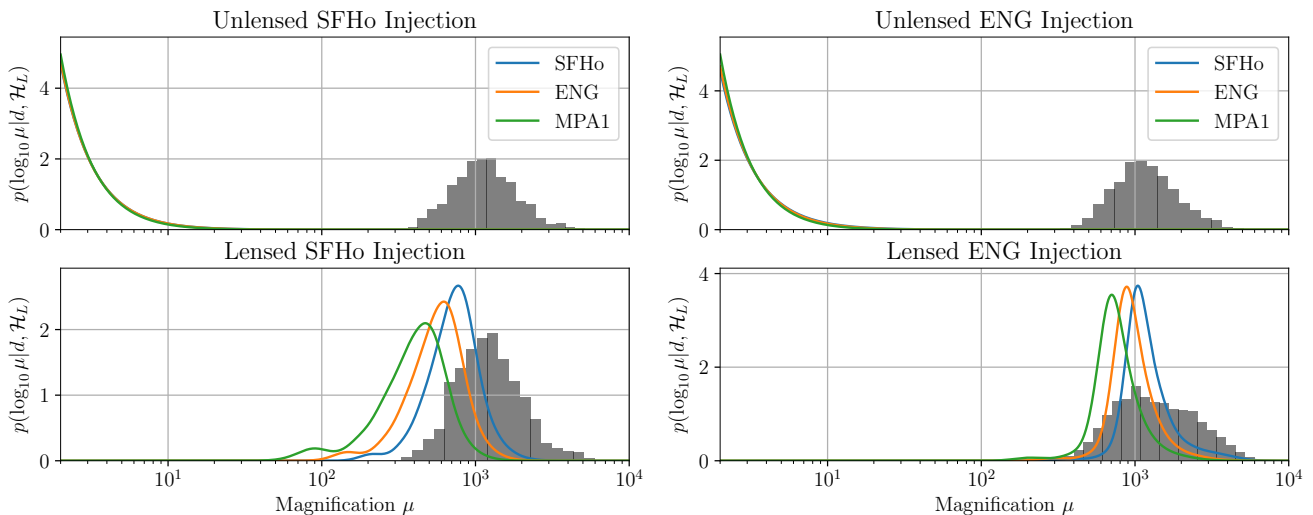


FIG. 5. Posterior distribution of magnifications inferred with posteriors of component masses and luminosity distance (gray bins) and that with posteriors of component masses and tidal deformability for given EOSs (colored line) with various injections. We show four different injections: Unlensed SFHo (top left), unlensed ENG (top right), lensed SFHo (bottom left) and lensed ENG (bottom right) injection. The posterior of the magnification μ inferred from the masses and from the tidal deformabilities are giving consistent results for lensed injections. Meanwhile, there exists tension between the posteriors recovered by the two means for unlensed injection. The injected BNS masses are ($m_1 = m_2 = 1.35 M_\odot$) and ($m_1 = m_2 = 2.02 M_\odot$) for the lensed and unlensed binaries, respectively. The binary neutron star is at an observed luminosity distance of $D^{\text{est}} = 100$ Mpc, with a signal-to-noise ratio of 31.

the posterior of the magnification μ rails against the prior instead of peaking at the true value (therefore $\mu = 1$), which result in the log Bayes factor $\log \mathcal{B}_U^L$ to be in different magnitude for the lensed and unlensed injections. As a supplementary analysis, we also performed the estimate on an injection set with a magnification of 100, finding that we can still disfavor lensing for the high-mass binary, but that we are unable to confirm lensing in this case (Appendix C).

V. BEYOND MOCK DATA: DISCUSSION

Our work demonstrates a robust methodology to rule out or confirm the gravitational lensing hypothesis for BNS mergers. The methodology can be used to rule out lensing for intrinsically high mass BNS events, or confirm it for the galactic double neutron star population. The mock data was produced for two different lensed and unlensed scenario, employing the SFHo and ENG equations of state consistent with the current GW and EM observations [78]. It is natural to wonder if the analysis could already rule out or confirm lensing for the high-mass binary neutron star event GW190425, and if not, what is required of a realistic detection to be able to make this distinction.

We evaluate the magnification posterior using both the mass estimate and the tidal deformability measurement (as in Sec. IV) for GW190425⁸, but find that both the lensed and unlensed magnification estimates overlap, allowing no clear

EOS	$\log \mathcal{B}_U^L$
SFHo	-0.610
ENG	-0.646
MPA1	-0.715

TABLE II. The log Bayes factor for the lensed hypothesis against unlensed hypothesis of GW190425 with various EOSs given.

constraints on the lens hypothesis (Fig. 6) The log Bayes factor for the lensed hypothesis against unlensed hypothesis are shown in Table II for a selected set of EOSs. We deduce that the magnification μ is less than 87.0, 86.5 and 75.3 for SFHo, ENG and MPA1, respectively, at a 99% confidence level.

However, had the event been observed at design sensitivity, and in the full detector network (LIGO Hanford/Livingston and Virgo), the network SNR would have been ~ 23 , which is much closer to the signal strengths which we used in our mock data simulations (SNR ~ 30). Therefore, while we can not set very stringent constraints on lensing for the GW190425 event. A similar event at a lower distance detected by LIGO/Virgo or the same event with more sensitive instruments, in the future, might allow us to probe the lensing hypothesis.

Moreover, we note that the lensing hypothesis can be ruled out more easily for higher mass events. The total mass of the GW190425 event was $3.4_{-0.1}^{+0.3} M_\odot$, which would already necessitate fairly large magnifications if it were lensed (Fig. 6). If the BNS population which produced GW190425 consists of higher mass BNS events, we will likely be able to set better constraints.

If the event is indeed lensed at a high magnification, then our method can be used to confirm that the event is lensed.

⁸ The parameter estimation samples released in [99] is used.

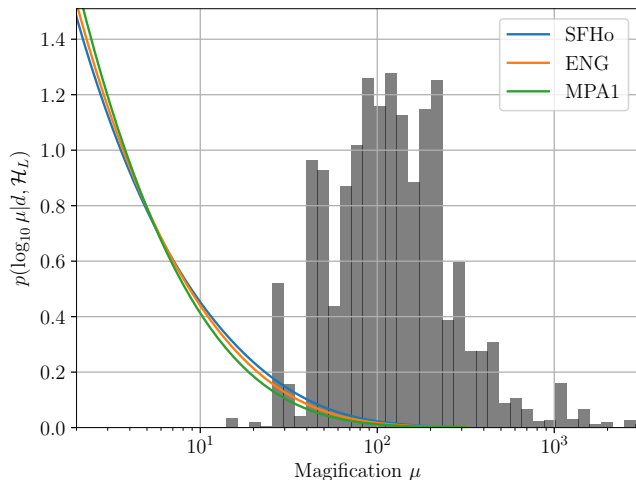


FIG. 6. Posterior distribution of magnifications inferred with the galactic double neutron star population assumed (gray bins) and posterior distribution of magnifications inferred with different EOSs assumed (colored lines). As the lensed and unlensed magnification estimates overlap, allowing no clear constraints on the lens hypothesis. We deduce that the magnification μ is less than 87.0, 86.5 and 75.3 for SFHo, ENG and MPA1, respectively, at a 99% confident.

It is currently unlikely that we will detect binary neutron star lensing within LIGO/Virgo. However, with future third-generation detectors such as the Einstein Telescope, lensed detections could be in the hundreds [27, 28]. We could discover these events at a much higher SNR than, allowing for more robust constraints than presented here.

As we observe more BNS events, we will be able to set more stringent constraints on the EOS of neutron stars due to the combination/stacking of multiple gravitational wave sources [59, 100] and their potential EM counterparts. Therefore, our estimate of the expected tidal deformabilities will improve, which in turn will allow for improved tests of the BNS lensing. Future studies employing populations of events will answer the above questions more definitively.

VI. CONCLUSIONS

If a GW from a BNS event is lensed, a combined measurement of the tidal effects and the binary masses of BNSs could be used to rule out or confirm the lensing hypothesis robustly. This test could be used to rule out lensing for intrinsically high-mass BNSs, similar to the recent GW190425 event. Lensed BNSs are one of the GW sources that can be gravitationally lensed and produce an electromagnetic counterpart. This makes them to an attractive target for multi-messenger studies. Indeed, lensed BNSs might allow for measurements of the Hubble constant [101], accurate tests of the speed of gravity [31, 33], various cosmography studies [102], and polarization tests [30]. Since our test could also be used to robustly confirm BNS lensing, it is expected to find several use-cases in these novel strong lensing avenues that utilize EM

counterparts.

ACKNOWLEDGMENTS

We thank Tjonnje Li, David Keitel, Ken Ng, Ajit Mehta, K. Haris, Chris Van Den Broeck, Christopher Berry and Shasvath Kapadia for their comments and suggestions. PTHP and OAH are supported by the research program of the Netherlands Organization for Scientific Research (NWO). TD acknowledges support by the European Union’s Horizon 2020 research and innovation program under grant agreement No 749145, BNSmergers. We are grateful for the computing resources provided by the LIGO-Caltech Computing Cluster where our analysis were carried out.

Appendix A: Gravitational-wave Parameter Estimation

The inner product of two real functions $a(t)$ and $b(t)$ are defined as

$$(a|b) = 4 \operatorname{Re} \int_{f_{\text{low}}}^{f_{\text{high}}} \frac{\tilde{a}(f)\tilde{b}^*(f)}{S_n(f)} df. \quad (\text{A1})$$

Here, $\tilde{a}(f)$ is the Fourier transform of $a(t)$, $*$ denotes complex conjugation and $S_n(f)$ denotes the one-sided power spectral density of the detector noise. f_{low} and f_{high} are the lower-cutoff and higher-cutoff frequency, respectively.

The posterior $p(\vec{\theta}|d)$ that a signal $h(\vec{\theta})$ with parameters $\vec{\theta}$ is embedded in a given data strain d , is given by

$$p(\vec{\theta}|d, \mathcal{H}) = \frac{\mathcal{L}(d|\vec{\theta}, \mathcal{H})p(\vec{\theta}|\mathcal{H})}{p(d|\mathcal{H})}. \quad (\text{A2})$$

To explore the posterior distribution in the high-dimensional parameter space, we employed the Nested Sampling algorithm as implemented in LALINFERENCE [97, 98].

Appendix B: Methods

In the lensing hypothesis \mathcal{H}_L , the magnification biases the intrinsic component masses m_i and luminosity distance D to their lensed counterparts. Accordingly, the inferred redshift will differ from the true value z .

We choose a power-law prior on the magnification and denote the PE-inferred quantities by m_i^{est} , D^{est} and z^{est} both in the lensed and unlensed case. Hence, the assumptions which hold under \mathcal{H}_L are

$$\begin{aligned} \mathcal{H}_L : p(\mu) &\propto \mu^{-3}, \\ D &= \sqrt{\mu} D^{\text{est}}, \\ z &= z(\sqrt{\mu} D^{\text{est}}), \\ m_i &= \frac{m_i^{\text{det}}}{1+z} = m_i^{\text{est}} \frac{1+z^{\text{est}}}{1+z}, \\ \Lambda_i^{\text{est}} &= \Lambda(m_i) = \Lambda\left(m_i^{\text{est}} \frac{1+z^{\text{est}}}{1+z}\right), \end{aligned} \quad (\text{B1})$$

while under the unlensed hypothesis \mathcal{H}_U one finds

$$\begin{aligned} \mathcal{H}_U : m_i &= m_i^{\text{est}}, \\ D &= D^{\text{est}}, \\ \Lambda_i^{\text{est}} &= \Lambda(m_i) = \Lambda(m_i^{\text{est}}). \end{aligned} \quad (\text{B2})$$

The priors on m^{est} and D^{est} under \mathcal{H}_L , given μ , are obtained by change of variables. By means of equations (B1) one has

$$\begin{aligned} p(D^{\text{est}}|\vec{\theta}, \mu, \mathcal{H}_L) &= p(D^*|\vec{\theta}, \mu, \mathcal{H}_L) \cdot \left| \frac{\partial D}{\partial D^{\text{est}}} \right|, \\ &= p(D^*|\vec{\theta}, \mu, \mathcal{H}_L) \cdot \mu^{1/2}. \end{aligned} \quad (\text{B3})$$

In the above, $\vec{\theta}$ represents all the binary parameters besides masses and distance and $D^* = D(D^{\text{est}}, \mu)$, as per the last one of equations (B1). The probability that an event at redshift $z = z(D)$ is lensed is measured by the optical depth:

$$\tau(z) = p(\mathcal{H}_L|z, \vec{\theta}, \mu). \quad (\text{B4})$$

The optical depth of lensing is [23]

$$\tau(z) = 4.17 \times 10^{-6} \left(\frac{D_c(z)}{\text{Gpc}} \right)^3 \quad (\text{B5})$$

where $D_c(z)$ is the comoving distance. Thus, one has

$$\begin{aligned} \tau(z)p(z|\vec{\theta}, \mu) &= p(\mathcal{H}_L, z|\vec{\theta}, \mu), \\ &\propto p(z|\vec{\theta}, \mu, \mathcal{H}_L). \end{aligned} \quad (\text{B6})$$

By means of equation (B6), equation (B3) becomes:

$$\begin{aligned} p(D^{\text{est}}|\vec{\theta}, \mu, \mathcal{H}_L) &= p(z^*|\vec{\theta}, \mu, \mathcal{H}_L) \cdot \left| \frac{\partial D}{\partial z} \right| \cdot \mu^{1/2}, \\ &\propto \tau(z^*)p(z^*|\vec{\theta}, \mu, \mathcal{H}_L) \cdot \left| \frac{\partial D}{\partial z} \right| \cdot \mu^{1/2}, \\ &\propto \tau(z^*)p(z^*|\mathcal{H}_L) \cdot \left| \frac{\partial D}{\partial z} \right| \cdot \mu^{1/2}. \end{aligned} \quad (\text{B7})$$

where $z^* = z(D^*)$ and we used the fact that the prior on z is independent of $\vec{\theta}$ and μ . In the same fashion, the lensed prior on the masses is:

$$\begin{aligned} p(m_1^{\text{est}}, m_2^{\text{est}}|D^{\text{est}}, \vec{\theta}, \mu, \mathcal{H}_L) &= p(m_1^*, m_2^*|D^{\text{est}}, \vec{\theta}, \mu, \mathcal{H}_L) \cdot \left| \frac{\partial(m_1, m_2)}{\partial(m_1^{\text{est}}, m_2^{\text{est}})} \right| \\ &= p(m_1^*, m_2^*|D^{\text{est}}, \vec{\theta}, \mu, \mathcal{H}_L) \cdot \left(\frac{1+z^{\text{est}}}{1+z^*} \right)^2, \end{aligned} \quad (\text{B8})$$

where $z^{\text{est}} = z(D^{\text{est}})$ and $m_i^* = m_i(m_i^{\text{est}}, z^{\text{est}}, z^*)$.

1. Magnification posterior with mass distributions

Here we demonstrate how one can estimate the magnification posterior of a given binary neutron star event, given that it comes from the galactic double neutron star population. For this purpose, we define the hypothesis $\mathcal{H}_L^{\text{DNS}}$ to refer to the magnification estimate from the binary *masses*. I.e., the mass prior $p(m_1, m_2|\mathcal{H}_L^{\text{DNS}})$ is the one for galactic double neutron stars, but we make no explicit constraint on the tidal measurements.

In the lensed hypothesis, the joint posterior inferred from a dataset d is:

$$\begin{aligned} p(\mu, D^{\text{est}}, m_1^{\text{est}}, m_2^{\text{est}}, \theta|d, \mathcal{H}_L^{\text{DNS}}) &= \mathcal{L}(D^{\text{est}}, m_1^{\text{est}}, m_2^{\text{est}}, \vec{\theta})p(\mu, D^{\text{est}}, m_1^{\text{est}}, m_2^{\text{est}}, \vec{\theta}|\mathcal{H}_L^{\text{DNS}}). \end{aligned} \quad (\text{B9})$$

Since the waveform model is unchanged, the likelihood \mathcal{L} is the same under both $\mathcal{H}_L^{\text{DNS}}$ and \mathcal{H}_U and does not depend on μ . The prior is:

$$\begin{aligned} & p(\mu, D^{\text{est}}, m_1^{\text{est}}, m_2^{\text{est}}, \vec{\theta} | \mathcal{H}_L^{\text{DNS}}) \\ &= p(m_1^{\text{est}}, m_2^{\text{est}} | D^{\text{est}}, \vec{\theta}, \mu, \mathcal{H}_L^{\text{DNS}}) p(D^{\text{est}} | \vec{\theta}, \mu, \mathcal{H}_L^{\text{DNS}}) \\ &\times p(\vec{\theta} | \mathcal{H}_L^{\text{DNS}}) p(\mu | \mathcal{H}_L^{\text{DNS}}), \end{aligned} \quad (\text{B10})$$

where we used the fact that $\vec{\theta}$ is independent of μ .

Inserting equation (B10) into expression (B9), we get:

$$\begin{aligned} & p(\mu, D^{\text{est}}, m_1^{\text{est}}, m_2^{\text{est}}, \vec{\theta} | d, \mathcal{H}_L^{\text{DNS}}) \\ &\propto \mathcal{L}(D^{\text{est}}, m_1^{\text{est}}, m_2^{\text{est}}, \vec{\theta}) p(m_1^{\text{est}}, m_2^{\text{est}} | D^{\text{est}}, \vec{\theta}, \mu, \mathcal{H}_L^{\text{DNS}}) \\ &\times p(D^{\text{est}} | \vec{\theta}, \mu, \mathcal{H}_L^{\text{DNS}}) p(\vec{\theta} | \mathcal{H}_L^{\text{DNS}}) p(\mu | \mathcal{H}_L^{\text{DNS}}). \end{aligned} \quad (\text{B11})$$

Similarly, the unlensed posterior samples are given by:

$$\begin{aligned} & p(D^{\text{est}}, m_1^{\text{est}}, m_2^{\text{est}}, \vec{\theta} | d, \mathcal{H}_U) \\ &\propto \mathcal{L}(D^{\text{est}}, m_1^{\text{est}}, m_2^{\text{est}}, \vec{\theta}) p(m_1^{\text{est}}, m_2^{\text{est}} | D^{\text{est}}, \vec{\theta}, \mathcal{H}_U) \\ &\times p(D^{\text{est}} | \vec{\theta}, \mathcal{H}_U) p(\vec{\theta} | \mathcal{H}_U). \end{aligned} \quad (\text{B12})$$

Therefore, one can rewrite equation (B11) as follows:

$$\begin{aligned} & p(\mu, D^{\text{est}}, m_1^{\text{est}}, m_2^{\text{est}}, \theta | d, \mathcal{H}_L^{\text{DNS}}) \\ &\propto p(D^{\text{est}}, m_1^{\text{est}}, m_2^{\text{est}}, \vec{\theta} | d, \mathcal{H}_U) p(\mu | \mathcal{H}_L^{\text{DNS}}) \\ &\times \frac{p(m_1^{\text{est}}, m_2^{\text{est}} | D^{\text{est}}, \vec{\theta}, \mu, \mathcal{H}_L^{\text{DNS}}) p(D^{\text{est}} | \vec{\theta}, \mu, \mathcal{H}_L^{\text{DNS}})}{p(m_1^{\text{est}}, m_2^{\text{est}} | D^{\text{est}}, \vec{\theta}, \mathcal{H}_U) p(D^{\text{est}} | \vec{\theta}, \mathcal{H}_U)} \\ &= p(D^{\text{est}}, m_1^{\text{est}}, m_2^{\text{est}}, \vec{\theta} | d, \mathcal{H}_U) \times \mathcal{W}, \end{aligned} \quad (\text{B13})$$

where we used the fact that $p(\vec{\theta} | \mathcal{H}_L^{\text{DNS}}) = p(\vec{\theta} | \mathcal{H}_U)$ and the terms in the numerator are computed as prescribed by equations (B7) and (B8).

Since the likelihood is unchanged, the weighting factor amounts to the prior ratio of the two scenarios,

$$\begin{aligned} \mathcal{W} &= \frac{p(m_1^{\text{est}}, m_2^{\text{est}} | D^{\text{est}}, \vec{\theta}, \mu, \mathcal{H}_L^{\text{DNS}}) p(\mu | \mathcal{H}_L^{\text{DNS}})}{p(m_1^{\text{est}}, m_2^{\text{est}} | D^{\text{est}}, \vec{\theta}, \mathcal{H}_U) p(D^{\text{est}} | \vec{\theta}, \mathcal{H}_U)} \\ &\times \tau(z^*) p(z^* | \mathcal{H}_L^{\text{DNS}}) \cdot \left| \frac{\partial D}{\partial z} \right| \cdot \mu^{1/2} \end{aligned} \quad (\text{B14})$$

We use a power-law prior on the magnification, $p(\mu | \mathcal{H}_L^{\text{DNS}}) \propto \mu^{-3}$ in [2, 6000]. Prior distributions on masses and distance for the lensed case are obtained from the unlensed ones by change of variables from the unlensed to the lensed quantities. The posterior samples and the priors under \mathcal{H}_U , in turn, are the ones of the LALInference analysis performed by the LIGO and Virgo Collaborations [3]. All the other binary parameters are unaffected by the lensing hypothesis and their priors cancel out in the weighting factor.

2. Magnification posterior with tidal measurements

To quantify the agreement between the measured tidal deformability and the estimated tidal deformability with a magnification given, we derive the posterior of the magnification $p(\mu | d, \text{EOS})$ with a given EOS as follows.

In the following derivation, the other parameters $\vec{\theta}$ are suppressed to ease the notation. In order to obtain the magnification via tidal measurement, we expand the posterior $p(\mu | d, \text{EOS})$ as

$$\begin{aligned} p(\mu | d, \text{EOS}, \mathcal{H}_L^{\text{Tidal}}) &= p(\mu | \mathcal{H}_L^{\text{Tidal}}) \int d\tilde{\Lambda} dm_i^{\text{det}} dD^{\text{est}} \\ &\times \mathcal{L}(d | \tilde{\Lambda}, m_i^{\text{det}}, D^{\text{est}}) \\ &\times p(\tilde{\Lambda}, m_i^{\text{det}}, D^{\text{est}} | \mu, \mathcal{H}_L, \text{EOS}) \\ &= p(\mu | \mathcal{H}_L^{\text{Tidal}}) \int d\tilde{\Lambda} dm_i^{\text{det}} dD^{\text{est}} \\ &\times \mathcal{L}(d | \tilde{\Lambda}, m_i^{\text{det}}, D^{\text{est}}) \\ &\times p(\tilde{\Lambda} | m_i^{\text{det}}, D^{\text{est}}, \mu, \mathcal{H}_L, \text{EOS}) \\ &\times p(m_i^{\text{det}}, D^{\text{est}} | \mu, \mathcal{H}_L, \text{EOS}). \end{aligned} \quad (\text{B15})$$

We notice that the tidal deformability is completely determined with a EOS and source-frame masses (therefore with detector-frame masses and luminosity distance given). Therefore $p(\tilde{\Lambda} | m_i^{\text{det}}, D^{\text{est}}, \mu, \mathcal{H}_L, \text{EOS}) = \delta(\tilde{\Lambda} - \tilde{\Lambda}^{\text{est}})$, where $\tilde{\Lambda}^{\text{est}}$ is the estimated tidal deformability. Therefore,

$$\begin{aligned} p(\mu | d, \text{EOS}, \mathcal{H}_L^{\text{Tidal}}) &= \int d\tilde{\Lambda} dm_i^{\text{det}} dD^{\text{est}} \mathcal{L}(d | \tilde{\Lambda}, m_i^{\text{det}}, D^{\text{est}}) \\ &\times \delta(\tilde{\Lambda} - \tilde{\Lambda}^{\text{est}}) p(m_i^{\text{det}}, D^{\text{est}} | \mu, \mathcal{H}_L, \text{EOS}) \\ &\times p(\mu | \mathcal{H}_L^{\text{Tidal}}) \\ &= \int dm_i^{\text{det}} dD^{\text{est}} \mathcal{L}(d | \tilde{\Lambda}^{\text{est}}, m_i^{\text{det}}, D^{\text{est}}) \\ &\times p(m_i^{\text{det}}, D^{\text{est}} | \mu, \mathcal{H}_L, \text{EOS}) p(\mu | \mathcal{H}_L^{\text{Tidal}}). \end{aligned} \quad (\text{B16})$$

As the likelihood is unchanged if we switch from $\mathcal{H}_L^{\text{Tidal}}$ and \mathcal{H}_U , we then express the likelihoods in terms of the posteriors under \mathcal{H}_U ,

$$\begin{aligned} p(\mu | d, \text{EOS}, \mathcal{H}_L^{\text{Tidal}}) &\propto \int dm_i^{\text{det}} dD^{\text{est}} \\ &\times \frac{p(\tilde{\Lambda}^{\text{est}}, m_i^{\text{det}}, D^{\text{est}} | d, \mathcal{H}_U)}{p(\tilde{\Lambda}^{\text{est}}, m_i^{\text{det}}, D^{\text{est}} | \mathcal{H}_U)} \\ &\times p(m_i^{\text{det}}, D^{\text{est}} | \mu, \mathcal{H}_L, \text{EOS}) p(\mu | \mathcal{H}_L^{\text{Tidal}}) \\ &= \int dm_i^{\text{det}} dD^{\text{est}} \\ &\times \frac{p(\tilde{\Lambda}^{\text{est}}, m_i^{\text{det}}, D^{\text{est}} | d, \mathcal{H}_U)}{p(\tilde{\Lambda}^{\text{est}} | m_i^{\text{det}}, D^{\text{est}}, \mathcal{H}_U)} \\ &\times \mathcal{W}_{\text{EOS}} \end{aligned} \quad (\text{B17})$$

In our study, we sample over the detector-frame masses and individual tidal deformability independently. Based on Eq. 4,

the prior $p(\tilde{\Lambda}^{\text{est}}|m_i^{\text{det}}, D^{\text{est}}, \mathcal{H}_U)$ is the same as the prior $p(\tilde{\Lambda}^{\text{est}}|q, \mathcal{H}_U)$, where $q \equiv m_2^{\text{det}}/m_1^{\text{det}}$.

$$\begin{aligned} p(\mu|d, \text{EOS}, \mathcal{H}_L^{\text{Tidal}}) &\propto \int dm_i^{\text{det}} dD^{\text{est}} \\ &\times \frac{p(\tilde{\Lambda}^{\text{est}}, m_i^{\text{det}}, D^{\text{est}}|d, \mathcal{H}_U)}{p(\tilde{\Lambda}^{\text{est}}|q, \mathcal{H}_U)} \mathcal{W}_{\text{EOS}} \\ &= \int dm_i^{\text{det}} dD^{\text{est}} p(m_i^{\text{det}}, D^{\text{est}}|d, \mathcal{H}_U) \\ &\times \frac{p(\tilde{\Lambda}^{\text{est}}|m_i^{\text{det}}, D^{\text{est}}, d, \mathcal{H}_U)}{p(\tilde{\Lambda}^{\text{est}}|q, \mathcal{H}_U)} \mathcal{W}_{\text{EOS}} \end{aligned} \quad (\text{B18})$$

And finally, we approximate the integral by an average over posterior samples. As a result,

$$p(\mu|d, \text{EOS}, \mathcal{H}_L^{\text{Tidal}}) \propto \left\langle \frac{p(\tilde{\Lambda}^{\text{est}}|d, \mathcal{H}_U)}{p(\tilde{\Lambda}^{\text{est}}|q, \mathcal{H}_U)} \mathcal{W}_{\text{EOS}} \right\rangle, \quad (\text{B19})$$

where $p(\tilde{\Lambda}^{\text{phase}}|d, \mathcal{H}_U)$ is the posterior distribution of the measured tidal deformability, $\tilde{\Lambda}^{\text{est}}$ is the estimated tidal deformability with a magnification and a EOS given. m_i^{det} and D^{est} are the observed component masses and the observed luminosity distance, respectively. The weight \mathcal{W}_{EOS} is given by

$$\begin{aligned} \mathcal{W}_{\text{EOS}} &= \frac{p(m_1^{\text{det}}, m_2^{\text{det}}|D^{\text{est}}, \mu, \mathcal{H}_L^{\text{Tidal}}, \text{EOS})p(D^{\text{est}}|\mu, \mathcal{H}_L^{\text{Tidal}})}{p(m_1^{\text{det}}, m_2^{\text{det}}|D^{\text{est}}, \mathcal{H}_U)p(D^{\text{est}}|\mathcal{H}_U)} \\ &\times p(\mu|\mathcal{H}_L^{\text{Tidal}}) \\ &= \frac{p(m_1^{\text{est}}, m_2^{\text{est}}|D^{\text{est}}, \mu, \mathcal{H}_L^{\text{Tidal}}, \text{EOS})p(D^{\text{est}}|\mu, \mathcal{H}_L^{\text{Tidal}})}{p(m_1^{\text{est}}, m_2^{\text{est}}|D^{\text{est}}, \mathcal{H}_U)p(D^{\text{est}}|\mathcal{H}_U)} \\ &\times p(\mu|\mathcal{H}_L^{\text{Tidal}}). \end{aligned} \quad (\text{B20})$$

The difference between \mathcal{W}_{EOS} and \mathcal{W} are the prior on $m_{1,2}^{\text{est}}$. For \mathcal{W}_{EOS} , the prior on $m_{1,2}^{\text{est}}$ is estimated based on a flat prior on the true source component mass to be uniform between $0.5M_\odot$ and the maximum mass allowed with a given EOS. While the Galactic double neutron star population is used for the calculation of \mathcal{W} in this paper.

Appendix C: Results with magnification μ of 100

In Fig. 7, we show the magnification posteriors evaluated with the two methods described in Sec IV with injections tabulated in Tab III given.

We observed that the required magnifications $p(\mu|d, \mathcal{H}_L^{\text{DNS}})$, as evaluated from the galactic double neutron star population, are in the $\mu \sim \mathcal{O}(10) - \mathcal{O}(1000)$ range for both the lensed and unlensed injections (Fig. 7, gray bins). Meanwhile, the magnifications as estimated from the unbiased tidal deformabilities are different for the two scenarios, favoring the unlensed case for the unlensed injection, and no clear preference for the lensed injection (solid lines, for the SFHo, ENG and MPA1 EOSs).

We find that the two magnification estimates disagree in the unlensed case, ruling out the lensed hypothesis at a log

EOS	Lensed ($\mu = 100$)	Unlensed ($\mu = 1$)
SFHo	(1.35, 432.94)	(1.58, 146.62)
ENG	(1.35, 644.66)	(1.58, 194.18)

TABLE III. Summary of the source-frame mass and the tidal deformability of the simulated binary neutron star mergers. Each cell shows the source-frame mass, tidal deformability pair (m, Λ) of the injection under different EOS and lensing scenario.

Bayes factor $\log \mathcal{B}_U^L$ of $-0.62(-0.68)$, $-0.77(-0.93)$ and $-1.04(-1.24)$ for SFHo, ENG and MPA1, respectively, for SFHo(ENG) injection. And overlap in the lensed case, showing no clear support on lensed hypothesis at a log Bayes factor $\log \mathcal{B}_U^L$ of $-0.07(0.13)$, $-0.08(0.77)$ and $-0.34(0.01)$ for SFHo, ENG and MPA1, respectively, for SFHo(ENG) injection.

These results show that the lensing hypothesis is disfavoured even for a weaker magnification with a weaker support. Meanwhile, the support for lensed hypothesis under lensed injection is too weak for us to give any statement for it.

-
- [1] B. P. Abbott et al. Advanced ligo. *Classical and Quantum Gravity*, 32(7):074001, mar 2015.
- [2] F. Acernese et al. Advanced virgo: a second-generation interferometric gravitational wave detector. *Classical and Quantum Gravity*, 32(2):024001, dec 2014.
- [3] B. P. Abbott et al. GWTC-1: A Gravitational-Wave Transient Catalog of Compact Binary Mergers Observed by LIGO and Virgo during the First and Second Observing Runs. *Phys. Rev.*, X9(3):031040, 2019.
- [4] LIGO Scientific Collaboration and Virgo Collaboration. https://gcn.gsfc.nasa.gov/lvc_events.html, 2019.
- [5] LIGO Scientific Collaboration and Virgo Collaboration. <https://gracedb.ligo.org/latest/>, 2019.
- [6] Kentaro Somiya. Detector configuration of KAGRA—the japanese cryogenic gravitational-wave detector. *Classical and Quantum Gravity*, 29(12):124007, jun 2012.
- [7] Yoichi Aso, Yuta Michimura, Kentaro Somiya, Masaki Ando, Osamu Miyakawa, Takanori Sekiguchi, Daisuke Tatsumi, and Hiroaki Yamamoto. Interferometer design of the kagra gravitational wave detector. *Phys. Rev. D*, 88:043007, Aug 2013.
- [8] T Akutsu, M Ando, S Araki, A Araya, T Arima, N Aritomi, H Asada, Y Aso, S Atsuta, K Awai, L Baiotti, M A Barton, D Chen, K Cho, K Craig, R DeSalvo, K Doi, K Eda, Y Enomoto, R Flaminio, S Fujibayashi, Y Fujii, M K Fujimoto, M Fukushima, T Furuhashi, and A Hagiwara. Construction of KAGRA: an underground gravitational-wave observatory. *Progress of Theoretical and Experimental Physics*, 2018(1), 01 2018. 013F01.
- [9] The LIGO Scientific Collaboration, the Virgo Collaboration,

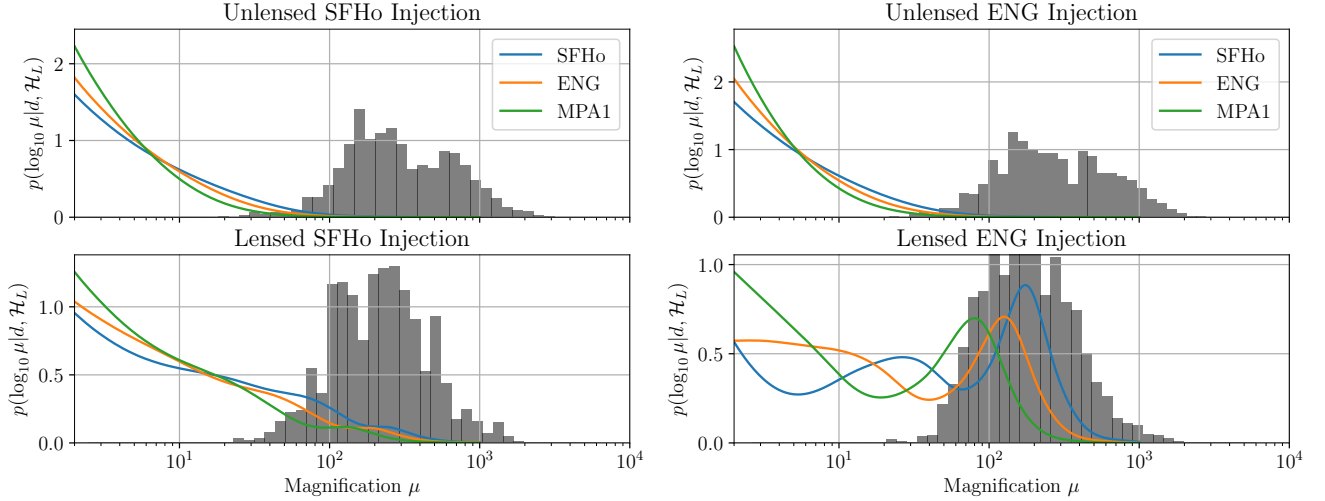


FIG. 7. Posterior distribution of magnifications inferred with posteriors of component masses and luminosity distance (gray bins) and that with posteriors of component masses and tidal deformability for given EOSs (colored line) with various injections. We show four different injections: Unlensed SFHo (top left), unlensed ENG (top right), lensed SFHo (bottom left) and lensed ENG (bottom right) injection. The posterior of the magnification μ inferred from the masses and from the tidal deformabilities are giving consistent results for lensed injections. Meanwhile, there exists tension between the posteriors recovered by the two means for unlensed injection. The injected BNS masses are ($m_1 = m_2 = 1.35 M_\odot$) and ($m_1 = m_2 = 1.58 M_\odot$) for the lensed and unlensed binaries, respectively. The binary neutron star is at an observed luminosity distance of $D^{\text{est}} = 100$ Mpc, with a signal-to-noise ratio of 25.

- and the KAGRA Collaboration. Prospects for observing and localizing gravitational-wave transients with advanced ligo, advanced virgo and kagra, 2013.
- [10] Hans C Ohanian. On the focusing of gravitational radiation. *International Journal of Theoretical Physics*, 9(6):425–437, 1974.
- [11] PV Bliokh and AA Minakov. Diffraction of light and lens effect of the stellar gravitation field. *Astrophysics and Space Science*, 34(2):L7–L9, 1975.
- [12] Robert J Bontz and Mark P Haugan. A diffraction limit on the gravitational lens effect. *Astrophysics and Space Science*, 78(1):199–210, 1981.
- [13] Kip S Thorne. The theory of gravitational radiation—an introductory review. In *Gravitational radiation*, pages 1–57, 1983.
- [14] Sh Deguchi and WD Watson. Diffraction in gravitational lensing for compact objects of low mass. *The Astrophysical Journal*, 307:30–37, 1986.
- [15] Takahiro T Nakamura. Gravitational lensing of gravitational waves from inspiraling binaries by a point mass lens. *Physical review letters*, 80(6):1138, 1998.
- [16] Ryuichi Takahashi and Takashi Nakamura. Wave effects in the gravitational lensing of gravitational waves from chirping binaries. *The Astrophysical Journal*, 595(2):1039–1051, Oct 2003.
- [17] Masamune Oguri. Strong gravitational lensing of explosive transients. *Reports on Progress in Physics*, 82(12):126901, Dec 2019.
- [18] Yun Wang, Albert Stebbins, and Edwin L. Turner. Gravitational lensing of gravitational waves from merging neutron star binaries. *Phys. Rev. Lett.*, 77:2875–2878, Sep 1996.
- [19] Liang Dai, Tejaswi Venumadhav, and Kris Sigurdson. Effect of lensing magnification on the apparent distribution of black hole mergers. *Phys. Rev. D*, 95:044011, Feb 2017.
- [20] Graham P. Smith, Mathilde Jauzac, John Veitch, Will M. Farr, Richard Massey, and Johan Richard. What if LIGO’s gravitational wave detections are strongly lensed by massive galaxy clusters? *Mon. Not. Roy. Astron. Soc.*, 475(3):3823–3828, 2018.
- [21] Graham P Smith, CPL Berry, Matteo Bianconi, Will M Farr, Mathilde Jauzac, RJ Massey, Johan Richard, Andrew Robertson, Keren Sharon, Alberto Vecchio, et al. Strong-lensing of gravitational waves by galaxy clusters. *arXiv preprint arXiv:1803.07851*, 2018.
- [22] M. Sereno, P. Jetzer, A. Sesana, and M. Volonteri. Cosmography with strong lensing of LISA gravitational wave sources. *MNRAS*, 415:2773–2781, August 2011.
- [23] K. Haris, Ajit Kumar Mehta, Sumit Kumar, Tejaswi Venumadhav, and Parameswaran Ajith. Identifying strongly lensed gravitational wave signals from binary black hole mergers. 2018.
- [24] Ken K. Y. Ng, Kaze W. K. Wong, Tom Broadhurst, and Tjonnie G. F. Li. Precise ligo lensing rate predictions for binary black holes. *Phys. Rev. D*, 97:023012, Jan 2018.
- [25] Shun-Sheng Li, Shude Mao, Yuetong Zhao, and Youjun Lu. Gravitational lensing of gravitational waves: a statistical perspective. *Monthly Notices of the Royal Astronomical Society*, 476(2):2220–2229, Feb 2018.
- [26] Masamune Oguri. Effect of gravitational lensing on the distribution of gravitational waves from distant binary black hole mergers. *MNRAS*, 480(3):3842–3855, Nov 2018.
- [27] Marek Biesiada, Xuheng Ding, Aleksandra Piórkowska, and Zong-Hong Zhu. Strong gravitational lensing of gravitational waves from double compact binaries—perspectives for the Einstein Telescope. *J. Cosmology Astropart. Phys.*, 2014(10):080, Oct 2014.
- [28] Xuheng Ding, Marek Biesiada, and Zong-Hong Zhu. Strongly lensed gravitational waves from intrinsically faint double compact binaries—prediction for the Einstein Telescope. *J. Cosmology Astropart. Phys.*, 2015(12):006, Dec 2015.
- [29] Kwun-Hang Lai, Otto A. Hannuksela, Antonio Herrera-

- Martín, Jose M. Diego, Tom Broadhurst, and Tjonnie G. F. Li. Discovering intermediate-mass black hole lenses through gravitational wave lensing. *Phys. Rev. D*, 98:083005, Oct 2018.
- [30] Katerina Chatzioannou, Nicolás Yunes, and Neil Cornish. Model-independent test of general relativity: An extended post-einsteinian framework with complete polarization content. *Phys. Rev. D*, 86:022004, Jul 2012.
- [31] Thomas E. Collett and David Bacon. Testing the speed of gravitational waves over cosmological distances with strong gravitational lensing. *Phys. Rev. Lett.*, 118:091101, Mar 2017.
- [32] Tessa Baker and Mark Trodden. Multimessenger time delays from lensed gravitational waves. *Phys. Rev. D*, 95:063512, Mar 2017.
- [33] Xi-Long Fan, Kai Liao, Marek Biesiada, Aleksandra Piórkowska-Kurpas, and Zong-Hong Zhu. Speed of gravitational waves from strongly lensed gravitational waves and electromagnetic signals. *Phys. Rev. Lett.*, 118:091102, Mar 2017.
- [34] H. Yu and F. Y. Wang. Testing weak equivalence principle with strongly lensed cosmic transients. *European Physical Journal C*, 78(9):692, Sep 2018.
- [35] Suvodip Mukherjee, Benjamin D. Wandelt, and Joseph Silk. Multi-messenger tests of gravity with weakly lensed gravitational waves. *arXiv e-prints*, page arXiv:1908.08950, Aug 2019.
- [36] Pierre Christian, Salvatore Vitale, and Abraham Loeb. Detecting stellar lensing of gravitational waves with ground-based observatories. *Phys. Rev. D*, 98:103022, Nov 2018.
- [37] Liang Dai, Shun-Sheng Li, Barak Zackay, Shude Mao, and Youjun Lu. Detecting lensing-induced diffraction in astrophysical gravitational waves. *Phys. Rev. D*, 98(10):104029, Nov 2018.
- [38] Alvin K. Y. Li, Rico K. L. Lo, Surabhi Sachdev, C. L. Chan, E. T. Lin, Tjonnie G. F. Li, and Alan J. Weinstein. Targeted Sub-threshold Search for Strongly-lensed Gravitational-wave Events. *arXiv e-prints*, page arXiv:1904.06020, Apr 2019.
- [39] Connor McIsaac, David Keitel, Thomas Collett, Ian Harry, Simone Mozzon, Oliver Edy, and David Bacon. Search for strongly lensed counterpart images of binary black hole mergers in the first two LIGO observing runs. *arXiv e-prints*, page arXiv:1912.05389, Dec 2019.
- [40] Pablo Marchant, Katelyn Breivik, Christopher P. L. Berry, Ilya Mandel, and Shane L. Larson. Eclipses of continuous gravitational waves as a probe of stellar structure. *Phys. Rev. D*, 101:024039, Jan 2020.
- [41] Tom Broadhurst, Jose M. Diego, and George Smoot III. Reinterpreting low frequency ligo/virgo events as magnified stellar-mass black holes at cosmological distances, 2018.
- [42] O. A. Hannuksela, K. Haris, K. K. Y. Ng, S. Kumar, A. K. Mehta, D. Keitel, T. G. F. Li, and P. Ajith. Search for gravitational lensing signatures in ligo-virgo binary black hole events. *The Astrophysical Journal*, 874(1):L2, Mar 2019.
- [43] B. P. Abbott et al. GW190425: Observation of a Compact Binary Coalescence with Total Mass $\sim 3.4M_{\odot}$, 2020.
- [44] Nicholas Farrow, Xing-Jiang Zhu, and Eric Thrane. The mass distribution of galactic double neutron stars. *The Astrophysical Journal*, 876(1):18, apr 2019.
- [45] Mohammadtaher Safarzadeh, Enrico Ramirez-Ruiz, and Edo Berger. GW190425 is inconsistent with being a binary neutron star born from a fast merging channel. *arXiv e-prints*, page arXiv:2001.04502, Jan 2020.
- [46] Graham P. Smith, Andrew Robertson, Matteo Bianconi, and Mathilde Jauzac. Discovery of strongly-lensed gravitational waves - implications for the lsst observing strategy, 2019.
- [47] Tim Dietrich, David Radice, Sebastiano Bernuzzi, Francesco Zappa, Albino Perego, Bernd Brügmann, Swami Vivekanandji Chaurasia, Reetika Dudi, Wolfgang Tichy, and Maximiliano Ujevic. CoRe database of binary neutron star merger waveforms. *Class. Quant. Grav.*, 35(24):24LT01, 2018.
- [48] A. Bauswein, H.T. Janka, K. Hebeler, and A. Schwenk. Equation-of-state dependence of the gravitational-wave signal from the ring-down phase of neutron-star mergers. *Phys.Rev.D*, 86:063001, 2012.
- [49] Kentaro Takami, Luciano Rezzolla, and Luca Baiotti. Constraining the equation of state of neutron stars from binary mergers. *Phys.Rev.Lett.*, 113(9):091104, 2014.
- [50] A. Bauswein, N. Stergioulas, and H.-T. Janka. Revealing the high-density equation of state through binary neutron star mergers. *Phys.Rev.D*, 90(2):023002, 2014.
- [51] Sebastiano Bernuzzi, Tim Dietrich, and Alessandro Nagar. Modeling the complete gravitational wave spectrum of neutron star mergers. *Phys.Rev.Lett.*, 115(9):091101, 2015.
- [52] Luciano Rezzolla and Kentaro Takami. Gravitational-wave signal from binary neutron stars: a systematic analysis of the spectral properties. *Phys.Rev.D*, 93(12):124051, 2016.
- [53] Ka Wa Tsang, Tim Dietrich, and Chris Van Den Broeck. Modeling the postmerger gravitational wave signal and extracting binary properties from future binary neutron star detections. *Phys.Rev.D*, 100(4):044047, 2019.
- [54] Tanja Hinderer, Benjamin D. Lackey, Ryan N. Lang, and Jocelyn S. Read. Tidal deformability of neutron stars with realistic equations of state and their gravitational wave signatures in binary inspiral. *Physical Review D*, 81(12), Jun 2010.
- [55] Thibault Damour and Alessandro Nagar. Relativistic tidal properties of neutron stars. *Phys.Rev.D*, 80:084035, 2009.
- [56] William G. Laarakkers and Eric Poisson. Quadrupole moments of rotating neutron stars. *Astrophys.J.*, 512:282–287, 1999.
- [57] Eric Poisson. Gravitational waves from inspiraling compact binaries: The quadrupole moment term. *Phys.Rev.D*, 57:5287–5290, 1998.
- [58] Ian Harry and Tanja Hinderer. Observing and measuring the neutron-star equation-of-state in spinning binary neutron star systems. *Class.Quant.Grav.*, 35(14):145010, 2018.
- [59] Michalis Agathos, Jeroen Meidam, Walter Del Pozzo, Tjonnie G. F. Li, Marco Tompitak, John Veitch, Salvatore Vitale, and Chris Van Den Broeck. Constraining the neutron star equation of state with gravitational wave signals from coalescing binary neutron stars. *Phys. Rev.*, D92(2):023012, 2015.
- [60] Anuradha Samajdar and Tim Dietrich. Waveform systematics for binary neutron star gravitational wave signals: Effects of spin, precession, and the observation of electromagnetic counterparts. *Phys. Rev.*, D100(2):024046, 2019.
- [61] Éanna É. Flanagan and Tanja Hinderer. Constraining neutron-star tidal love numbers with gravitational-wave detectors. *Physical Review D*, 77(2), Jan 2008.
- [62] Tanja Hinderer, Benjamin D. Lackey, Ryan N. Lang, and Jocelyn S. Read. Tidal deformability of neutron stars with realistic equations of state and their gravitational wave signatures in binary inspiral. *Phys. Rev. D*, 81:123016, Jun 2010.
- [63] P. A. R. Ade et al. Planck 2013 results. XVI. Cosmological parameters. *Astron. Astrophys.*, 571:A16, 2014.
- [64] Liang Dai and Tejaswi Venumadhav. On the waveforms of gravitationally lensed gravitational waves. *arXiv e-prints*, page arXiv:1702.04724, Feb 2017.
- [65] C. Messenger and J. Read. Measuring a cosmological distance-redshift relationship using only gravitational wave

- observations of binary neutron star coalescences. *Phys. Rev. Lett.*, 108:091101, Feb 2012.
- [66] Roger Blandford and Ramesh Narayan. Fermat’s Principle, Caustics, and the Classification of Gravitational Lens Images. *ApJ*, 310:568, Nov 1986.
- [67] L. Engvik, E. Osnes, M. Hjorth-Jensen, G. Bao, and E. Osgaard. Asymmetric Nuclear Matter and Neutron Star Properties. *ApJ*, 469:794, Oct 1996.
- [68] Soumi De, Daniel Finstad, James M. Lattimer, Duncan A. Brown, Edo Berger, and Christopher M. Biwer. Tidal Deformabilities and Radii of Neutron Stars from the Observation of GW170817. *Phys. Rev. Lett.*, 121(9):091102, 2018. [Erratum: *Phys. Rev. Lett.* 121,no.25,259902(2018)].
- [69] Andreas Bauswein, Oliver Just, Hans-Thomas Janka, and Nikolaos Stergioulas. Neutron-star radius constraints from GW170817 and future detections. *Astrophys. J.*, 850(2):L34, 2017.
- [70] Ben Margalit and Brian D. Metzger. Constraining the Maximum Mass of Neutron Stars From Multi-Messenger Observations of GW170817. *Astrophys. J.*, 850(2):L19, 2017.
- [71] Elias R. Most, Lukas R. Weih, Luciano Rezzolla, and Jürgen Schaffner-Bielich. New constraints on radii and tidal deformabilities of neutron stars from GW170817. *Phys. Rev. Lett.*, 120(26):261103, 2018.
- [72] Michael W Coughlin, Tim Dietrich, Zoheyr Doctor, Daniel Kasen, Scott Coughlin, Anders Jerkstrand, Giorgos Leloudas, Owen McBrien, Brian D Metzger, Richard O’Shaughnessy, and Stephen J Smartt. Constraints on the neutron star equation of state from at2017gfo using radiative transfer simulations. *Monthly Notices of the Royal Astronomical Society*, 480(3):3871–3878, 2018.
- [73] Michael W Coughlin, Tim Dietrich, Ben Margalit, and Brian D Metzger. Multimessenger Bayesian parameter inference of a binary neutron star merger. *Monthly Notices of the Royal Astronomical Society: Letters*, 489(1):L91–L96, 08 2019.
- [74] David Radice and Liang Dai. Multimessenger Parameter Estimation of GW170817. *Eur. Phys. J.*, A55(4):50, 2019.
- [75] Eemeli Annala, Tyler Gorda, Alekski Kurkela, and Alekski Vuorinen. Gravitational-wave constraints on the neutron-star-matter Equation of State. *Phys. Rev. Lett.*, 120(17):172703, 2018.
- [76] Collin D. Capano, Ingo Tews, Stephanie M. Brown, Ben Margalit, Soumi De, Sumit Kumar, Duncan A. Brown, Badri Krishnan, and Sanjay Reddy. GW170817: Stringent constraints on neutron-star radii from multimessenger observations and nuclear theory. 2019.
- [77] H. Thankful Cromartie et al. Relativistic Shapiro delay measurements of an extremely massive millisecond pulsar. *Nat. Astron.*, 4(1):72–76, 2019.
- [78] David Radice, Albino Perego, Francesco Zappa, and Sebastiano Bernuzzi. GW170817: Joint Constraint on the Neutron Star Equation of State from Multimessenger Observations. *Astrophys. J.*, 852(2):L29, 2018.
- [79] B. P. Abbott et al. GW170817: Observation of Gravitational Waves from a Binary Neutron Star Inspiral. *Phys. Rev. Lett.*, 119(16):161101, 2017.
- [80] B. P. Abbott, R. Abbott, T. D. Abbott, F. Acernese, K. Ackley, C. Adams, T. Adams, P. Addesso, R. X. Adhikari, V. B. Adya, and et al. Multi-messenger observations of a binary neutron star merger. *The Astrophysical Journal*, 848(2):L12, Oct 2017.
- [81] Iair Arcavi, Curtis McCully, Griffin Hosseinzadeh, D. Andrew Howell, Sergiy Vasylyev, Dovi Poznanski, Michael Zaltzman, Dan Maoz, Leo Singer, Stefano Valenti, Daniel Kasen, Jennifer Barnes, Tsvi Piran, and Wen-fai Fong. Optical Follow-up of Gravitational-wave Events with Las Cumbres Observatory. *ApJ*, 848(2):L33, Oct 2017.
- [82] R. Chornock et al. The Electromagnetic Counterpart of the Binary Neutron Star Merger LIGO/VIRGO GW170817. IV. Detection of Near-infrared Signatures of r-process Nucleosynthesis with Gemini-South. *Astrophys. J.*, 848(2):L19, 2017.
- [83] D. A. Coulter, R. J. Foley, C. D. Kilpatrick, M. R. Drout, A. L. Piro, B. J. Shappee, M. R. Siebert, J. D. Simon, N. Ulloa, D. Kasen, and et al. Swope supernova survey 2017a (sss17a), the optical counterpart to a gravitational wave source. *Science*, 358(6370):1556–1558, Oct 2017.
- [84] M. R. Drout, A. L. Piro, B. J. Shappee, C. D. Kilpatrick, J. D. Simon, C. Contreras, D. A. Coulter, R. J. Foley, M. R. Siebert, N. Morrell, and et al. Light curves of the neutron star merger gw170817/sss17a: Implications for r-process nucleosynthesis. *Science*, 358(6370):1570–1574, Oct 2017.
- [85] P. A. Evans, S. B. Cenko, J. A. Kennea, S. W. K. Emery, N. P. M. Kuin, O. Korobkin, R. T. Wollaeger, C. L. Fryer, K. K. Madsen, F. A. Harrison, and et al. Swiftandnustarobservations of gw170817: Detection of a blue kilonova. *Science*, 358(6370):1565–1570, Oct 2017.
- [86] G. Hallinan, A. Corsi, K. P. Mooley, K. Hotokezaka, E. Nakar, M. M. Kasliwal, D. L. Kaplan, D. A. Frail, S. T. Myers, T. Murphy, and et al. A radio counterpart to a neutron star merger. *Science*, 358(6370):1579–1583, Oct 2017.
- [87] M. M. Kasliwal, E. Nakar, L. P. Singer, D. L. Kaplan, D. O. Cook, A. Van Sistine, R. M. Lau, C. Fremling, O. Gottlieb, J. E. Jencson, and et al. Illuminating gravitational waves: A concordant picture of photons from a neutron star merger. *Science*, 358(6370):1559–1565, Oct 2017.
- [88] A. Murguía-Berthier, E. Ramirez-Ruiz, C. D. Kilpatrick, R. J. Foley, D. Kasen, W. H. Lee, A. L. Piro, D. A. Coulter, M. R. Drout, B. F. Madore, and et al. A neutron star binary merger model for gw170817/grb 170817a/sss17a. *The Astrophysical Journal*, 848(2):L34, Oct 2017.
- [89] M. Nicholl et al. The Electromagnetic Counterpart of the Binary Neutron Star Merger LIGO/VIRGO GW170817. III. Optical and UV Spectra of a Blue Kilonova From Fast Polar Ejecta. *Astrophys. J.*, 848(2):L18, 2017.
- [90] S. J. Smartt, T.-W. Chen, A. Jerkstrand, M. Coughlin, E. Kankare, S. A. Sim, M. Fraser, C. Inserra, K. Maguire, K. C. Chambers, and et al. A kilonova as the electromagnetic counterpart to a gravitational-wave source. *Nature*, 551(7678):75–79, Oct 2017.
- [91] M. Soares-Santos, D. E. Holz, J. Annis, R. Chornock, K. Herner, E. Berger, D. Brout, H.-Y. Chen, R. Kessler, M. Sako, and et al. The electromagnetic counterpart of the binary neutron star merger ligo/virgo gw170817. i. discovery of the optical counterpart using the dark energy camera. *The Astrophysical Journal*, 848(2):L16, Oct 2017.
- [92] N. R. Tanvir, A. J. Levan, C. González-Fernández, O. Korobkin, I. Mandel, S. Rosswog, J. Hjorth, P. D’Avanzo, A. S. Fruchter, C. L. Fryer, T. Kangas, B. Milvang-Jensen, S. Rosetti, D. Steeghs, R. T. Wollaeger, Z. Cano, C. M. Copperwheat, S. Covino, V. D’Elia, A. de Ugarte Postigo, P. A. Evans, W. P. Even, S. Fairhurst, R. Figuera Jaimes, C. J. Fontes, Y. I. Fujii, J. P. U. Fynbo, B. P. Gompertz, J. Greiner, G. Hodosan, M. J. Irwin, P. Jakobsson, U. G. Jørgensen, D. A. Kann, J. D. Lyman, D. Malesani, R. G. McMahon, A. Melandri, P. T. O’Brien, J. P. Osborne, E. Palazzi, D. A. Perley, E. Pian, S. Piranomonte, M. Rabus, E. Rol, A. Rowlinson, S. Schulze, P. Sutton, C. C. Thöne, K. Ulaczyk, D. Watson, K. Wiersema, and R. A. M. J. Wijers. The Emergence of a

- Lanthanide-rich Kilonova Following the Merger of Two Neutron Stars. *ApJ*, 848(2):L27, Oct 2017.
- [93] Masaomi Tanaka, Yousuke Utsumi, Paolo A. Mazzali, Nozomu Tominaga, Michitoshi Yoshida, Yuichiro Sekiguchi, Tomoki Morokuma, Kentaro Motohara, Kouji Ohta, Koji S. Kawabata, and et al. Kilonova from post-merger ejecta as an optical and near-infrared counterpart of gw170817. *Publications of the Astronomical Society of Japan*, 69(6), Oct 2017.
- [94] E. Troja, L. Piro, H. van Eerten, R. T. Wollaeger, M. Im, O. D. Fox, N. R. Butler, S. B. Cenko, T. Sakamoto, C. L. Fryer, and et al. The x-ray counterpart to the gravitational-wave event gw170817. *Nature*, 551(7678):71–74, Oct 2017.
- [95] Keith C. Gendreau, Zaven Arzoumanian, and Takashi Oka-jima. The Neutron star Interior Composition Explorer (NICER): an Explorer mission of opportunity for soft x-ray timing spectroscopy. In Tadayuki Takahashi, Stephen S. Murray, and Jan-Willem A. den Herder, editors, *Space Telescopes and Instrumentation 2012: Ultraviolet to Gamma Ray*, volume 8443, pages 322 – 329. International Society for Optics and Photonics, SPIE, 2012.
- [96] A. W. Steiner, M. Hempel, and T. Fischer. CORE-COLLAPSE SUPERNOVA EQUATIONS OF STATE BASED ON NEUTRON STAR OBSERVATIONS. *The Astrophysical Journal*, 774(1):17, aug 2013.
- [97] J. Veitch et al. Parameter estimation for compact binaries with ground-based gravitational-wave observations using the LAL-Inference software library. *Phys. Rev.*, D91(4):042003, 2015.
- [98] LIGO Scientific Collaboration. LIGO Algorithm Library - LALSuite. free software (GPL), 2018.
- [99] LIGO Scientific Collaboration and Virgo Collaboration. <https://dcc.ligo.org/LIGO-P2000026/public>, 2020.
- [100] Walter Del Pozzo, Tjonnie G. F. Li, Michalis Agathos, Chris Van Den Broeck, and Salvatore Vitale. Demonstrating the feasibility of probing the neutron star equation of state with second-generation gravitational wave detectors. *Phys. Rev. Lett.*, 111(7):071101, 2013.
- [101] Kai Liao, Xi-Long Fan, Xuheng Ding, Marek Biesiada, and Zong-Hong Zhu. Precision cosmology from future lensed gravitational wave and electromagnetic signals. *Nature Communications*, 8(1), Oct 2017.
- [102] G P Smith, M Bianconi, M Jauzac, J Richard, A Robertson, C P L Berry, R Massey, K Sharon, W M Farr, and J Veitch. Deep and rapid observations of strong-lensing galaxy clusters within the sky localization of gw170814. *Monthly Notices of the Royal Astronomical Society*, 485(4):5180–5191, Mar 2019.